

## MIT Open Access Articles

*Selective Sulfidation and Electrowinning of Nickel  
and Cobalt for Lithium Ion Battery Recycling*

The MIT Faculty has made this article openly available. **Please share**  
how this access benefits you. Your story matters.

**Citation:** Stinn, Caspar and Antoine Allanore. "Selective Sulfidation and Electrowinning of Nickel and Cobalt for Lithium Ion Battery Recycling." Ni-Co 2021: The 5th International Symposium on Nickel and Cobalt, March 2021, virtual event, Springer, February 2021. © 2021 The Minerals, Metals & Materials Society

**As Published:** [http://dx.doi.org/10.1007/978-3-030-65647-8\\_7](http://dx.doi.org/10.1007/978-3-030-65647-8_7)

**Publisher:** Springer International Publishing

**Persistent URL:** <https://hdl.handle.net/1721.1/131162>

**Version:** Author's final manuscript: final author's manuscript post peer review, without publisher's formatting or copy editing

**Terms of use:** Creative Commons Attribution-Noncommercial-Share Alike



# Selective Sulfidation and Electrowinning of Nickel and Cobalt for Lithium Ion Battery Recycling

Caspar Stinn<sup>1</sup> and Antoine Allanore<sup>1+</sup>

1. Massachusetts Institute of Technology, Department of Materials Science and Engineering,  
77 Massachusetts Ave, Cambridge, MA, USA 02139

+ Corresponding Author: allanore@mit.edu

## Abstract

Processes for recycling lithium ion batteries (LIB), in particular complex chemistries such as those containing nickel-manganese-cobalt oxide (NMC) cathodes, are hindered by tradeoffs between capital cost, process sustainability, and materials recovery. Most metal separations in primary and secondary production of critical elements rely on anion exchange chemistries. Herein, we explore the application of a novel oxide-sulfide anion exchange methodology to facilitate LIB recycling. Beginning with selective sulfidation of NMC cathode oxides, we demonstrate that lithium may be stabilized as a sulfate, manganese as an oxysulfide, and nickel and cobalt as sulfides from the mixed metal feed, potentially facilitating isolation of lithium via leaching and nickel-cobalt via flotation. Following, we explore molten sulfide electrolysis as a method of process intensification, combining separation and reduction into a single unit operation for difficult to separate metals such as cobalt and nickel. We demonstrate selective reduction of cobalt from mixed nickel-cobalt sulfide, as produced in selective sulfidation of waste NMC cathodes, using a barium-lanthanum sulfide supporting electrolyte. Our preliminary results suggest that selective sulfidation as a pretreatment for selective molten sulfide electrolysis is a promising avenue for separation of critical elements from complicated materials feeds, such as those found in lithium ion battery recycling streams.

**Keywords:** Nickel, Cobalt, Lithium-ion battery, NMC cathode, Sulfidation, Electrolysis, Recycling, Molten sulfide, Sustainability

## Introduction

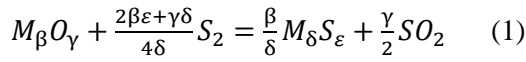
Increasing demand for electric vehicles has the potential to strain geopolitically-sensitive supply chains of battery-grade materials, such as cobalt, motivating efforts to develop recycling technologies to recycle and reuse strategic elements<sup>1</sup>. While a variety of pyrometallurgical, hydrometallurgical, and direct recycling processes have been considered for recovery of critical battery materials, present methodologies are plagued by tradeoffs between capital cost, process sustainability, and materials recovery, with additional complications arising from non-standardized chemistries that exhibit inherent, thermodynamic difficulties in separation<sup>2,3</sup>. For recycling of lithium ion batteries (LIB) containing nickel-manganese-cobalt-based (NMC) cathodes, challenges arise from the fact that nickel, manganese, cobalt, and lithium within the cathode exist as mixed-metal oxide compounds and solid solutions<sup>4,5</sup>; thus separation of lithium, nickel, manganese, and cobalt presently requires chemical methods to isolate individual elements. Chemical separation of metallic elements is often rooted in anion exchange, where the anion of a metal compound, or in the case of liquid-liquid hydrometallurgy the anionic solvating or chelating species, is exchanged with another to facilitate separation based on property differences between the phases containing different anions. Conventional primary and secondary processing technologies for battery metals including matte smelting<sup>6</sup>, carbochlorination<sup>7</sup>, and solvent extraction<sup>8,9</sup> can all be viewed in the framework of anion exchange.

Herein, we consider an oxide-sulfide-based anion exchange chemistry and its potential to handle the multi-element nature of LIB recycling streams. Oxide-sulfide-based anion exchange for battery elements has previously been considered in the context of selective sulfidation of nickel oxides to sulfides<sup>10</sup> and selective sulfation of nickel and cobalt oxides to sulfates<sup>11,12</sup>. Sulfidation supports separation of oxides from sulfides via froth flotation<sup>10</sup> and sulfation supports separation of oxides from sulfates via leaching<sup>11,12</sup>. Meanwhile, sulfide chemistry allows for economically competitive<sup>13</sup>, environmentally sustainable<sup>14</sup>, and selective<sup>15</sup> metal reduction via molten sulfide electrolysis. Through

demonstration of selective sulfidation and selective molten sulfide electrolytic reduction of NMC battery cathode metals, we establish the foundation of a sulfide-based processing route for lithium ion battery recycling.

### Thermodynamic Basis for Selective Sulfidation and Molten Sulfide Electrolytic Reduction

For the generic sulfidation reaction of a metal (M) oxide (Eq 1), through the law of mass action and the van't Hoff equation, a critical sulfur to sulfur dioxide partial pressure ratio,  $[P_{S_2}/P_{SO_2}]_{crit}$ , can be defined for thermodynamic spontaneity of Eq. 1 at equilibrium (Eq 2), where R is the gas constant, T is the absolute temperature, a is the compound activity, P is the gas partial pressure, and  $\beta$ ,  $\gamma$ ,  $\delta$ ,  $\varepsilon$  are stoichiometric coefficients:



$$\left[ \frac{P_{S_2}^{\frac{2\beta\varepsilon + \gamma\delta}{4\delta}}}{P_{SO_2}^{\frac{\gamma}{2}}} \right]_{crit} = e^{\frac{\Delta G_T^{\circ}}{RT}} \frac{a_{M_{\delta}S_{\varepsilon}}^{\frac{\beta}{\delta}}}{a_{M_{\beta}O_{\gamma}}^{\frac{\beta}{\delta}}} \quad (2)$$

Similar relations to Eq. 2 can be defined for the reactions between the metal, oxides, oxysulfides, sulfates, and sulfides. Assuming the metal and its compounds are non-volatile, for a gas phase consisting only of oxygen and sulfur containing species at a given temperature and total pressure,  $P_{SO_2}$  is a monotonic function of  $P_{S_2}$ , thereby defining the  $P_{S_2}/P_{SO_2}$  ratio as a monotonic function of  $P_{S_2}$ . When the condensed metal compound reactant and product phases are soluble, their activities at a given  $P_{S_2}/P_{SO_2}$  ratio may be related to one another through the Gibbs-Duhem equation. Assuming insoluble reactant and product metal compounds at unit activity, Eq. 2 converges to a Kellogg formalism. The stability of cobalt and its oxides and sulfides at 1000 °C as a function of gas atmosphere is depicted in the Kellogg diagram of Figure 1a. Following a similar formalism for nickel, manganese, and lithium, a sulfidation series may be defined for sulfidation of nickel, manganese, cobalt, and lithium oxides (Figure 1b). While actual nickel-manganese-cobalt oxide (NMC) lithium ion battery (LIB) cathodes are composed of multi-metal oxide compounds and solid solutions, the activity ratio of pure metal oxides within single phases of NMC cathodes is far outweighed by their respective  $P_{S_2}/P_{SO_2}$  ratios differences. This suggests that a sulfidation series composed of pure end-member oxides is a suitable first-pass indication of sulfidation

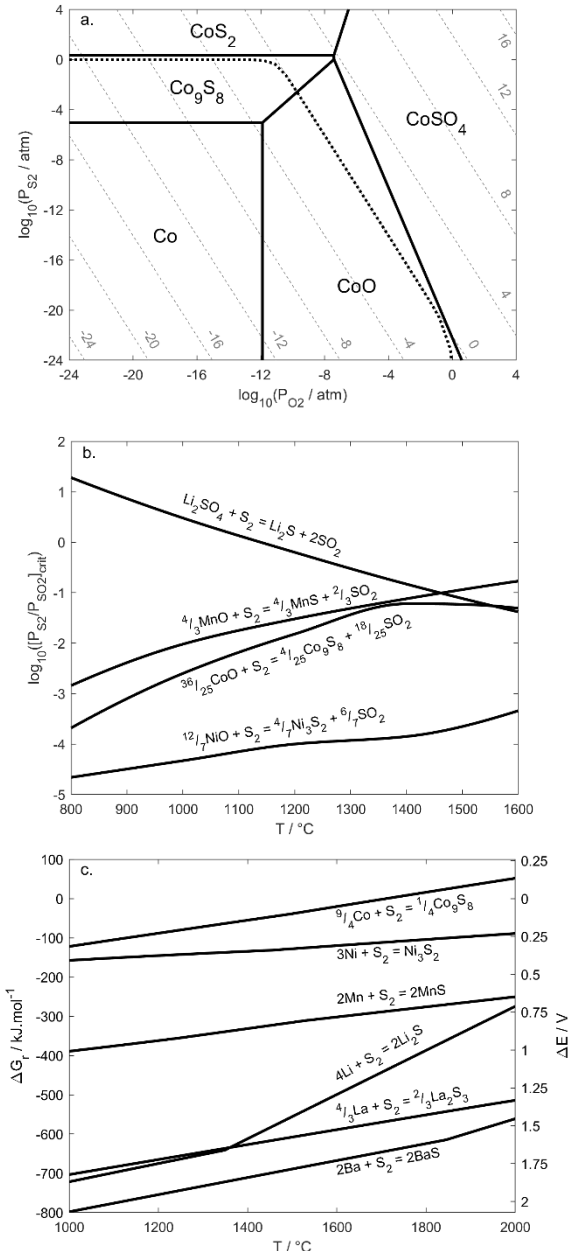


**Figure 1: Oxide-sulfide-based anion exchange chemistry offers selective separation opportunities for battery metals.** a. A Kellogg formalism, shown here for cobalt at 1000 °C, can be used to determine a critical gas atmosphere for sulfidation to occur. b. Comparison of critical gas ratios for sulfidation allows for construction of a sulfidation series, shown here for battery metals. c. Ellingham comparison of the reduction selectivity of battery metal sulfides and sulfide supporting electrolytes, suggesting that molten sulfide electrolysis may be selective for critical battery elements.

selectivity. As predicted in Figure 1b, during sulfidation of a NMC cathode, lithium may be stabilized as a sulfate, while nickel, cobalt, and manganese may be individually stabilized as either oxides or sulfides. Such outcome opens recovery methods for NMC cathode elements including leaching of lithium sulfate and froth flotation to separate nickel, cobalt, and manganese. This may be facilitated by oxide-sulfide anion exchange.

Molten sulfide electrolysis is a potential process intensification to integrate separation and reduction of mixed metal sulfides resulting from selective sulfidation. For the generic metal sulfidation reaction (Eq. 3), the corresponding decomposition potential ( $\Delta E$ ) may be found using the Nernst equation (Eq. 4), where  $\Delta G_r^\circ$  is the standard Gibbs energy,  $z$  is the number of electrons involved in the reaction (for 1 mole of  $S_2$ ,  $z = 4$ ),  $F$  is the Faraday constant, and  $\beta$ ,  $\gamma$  are stoichiometric coefficients.



$$\Delta E = \frac{-\Delta G_r^\circ}{zF} - \frac{RT}{zF} \ln \left( \frac{a_{M_\beta S_\gamma}^{\frac{2}{\gamma}}}{P_{S_2} a_M^{\frac{2\beta}{\gamma}}} \right) \quad (4)$$

Following an Ellingham formalism for pure species at unit activity under a pure sulfur atmosphere, a reduction series may be tabulated for NMC cathode endmember sulfides, as well as supporting electrolytes<sup>14–16</sup> for molten sulfide electrolysis (Figure 1c). While the solution thermodynamics of relevant molten sulfides are under development, review of the decomposition voltages between pure species suggests that molten sulfide electrolysis at 1500 °C is a promising approach for selective reduction of nickel, manganese, cobalt, and lithium sulfides using a barium-lanthanum sulfide supporting electrolyte, due to the large relative difference in decomposition potential between species. In the following sections, we demonstrate selective sulfidation of NMC cathode oxides and selective molten sulfide electrolysis, constituting an integrated sulfidation-electrolytic NMC cathode recycling pathway.

## Selective Sulfidation of Nickel-Manganese-Cobalt Oxide Cathodes

### Experimental

Simulated nickel-manganese-cobalt (NMC) oxide cathode material ( $\text{LiNi}_{1/3}\text{Mn}_{1/3}\text{Co}_{1/3}\text{O}_2$ , 98% purity, Sigma Aldrich) was used as the oxide precursor for selective sulfidation experiments. While industrially  $\text{H}_2\text{S}$  and  $\text{CS}_2$  are commonly employed for sulfidation of oxides, their use for complete sulfidation of mixed transition metal oxide catalysts<sup>17</sup> calls into question the suitability of  $\text{H}_2\text{S}$  and  $\text{CS}_2$  for selective sulfidation. Therefore, vaporized elemental sulfur ( $S_x$ , 99.5%, purity, Acros Organics) served as the sulfidizing agent. At temperatures above 800°C, sulfur gas is predominantly diatomic<sup>18</sup>. Selective sulfidation of metals from the mixed Li-Ni-Mn-Co oxide was conducted in a packed bed reactor, consisting of a 20 mm OD, 14 mm ID crucible fabricated in-house from machinable alumina ( $\text{Al}_2\text{O}_3$ , 96% purity, Rescor 960, Cotronics Corp), with seven 1 mm diameter holes spaced 2 mm apart drilled through the bottom of the crucible to support sulfur gas flow to the oxide. NMC oxide powder was loaded into the alumina crucible at a porosity of 90%, at a sulfidation charge of 2 g of oxide. Care was taken to avoid loss of the oxide precursor through the bottom crucible holes. The alumina crucible was held in the hot zone of a vertical tube furnace (SS15R-2.50X6V- 1Z, Mellen) within an alumina tube (25mm OD, 21 mm ID). Leveraging the thermal gradient of the tube furnace, sulfur gas was boiled from a 316 stainless steel crucible held below the alumina crucible, with sulfur gas transported to the oxide-containing crucible via an argon (Ar, 99.95% purity, Air Gas) carrier gas flowing at 1000 sccm. Sulfidation conversion was monitored by measuring the rate of  $\text{SO}_2$  generation via IR gas analysis (IR208, Infrared Industries) of the product gas stream. Sulfur gas flowrate was similarly monitored using an  $\text{H}_2\text{S}$  tracer calibrated to sulfur evaporation rate. The sulfidized NMC was mounted in epoxy, cross sectioned, polished, and then imaged optically and via scanning electron microscope (SEM, JEOL JSM-6610LV, JEOL Ltd.) equipped with an energy dispersion spectroscopy analyzer (EDS, Sirius SD detector, SGX Sensortech Ltd.). To determine the extent of sulfidation of lithium oxide from the NMC, x-ray diffraction analysis (XRD) was conducted on crushed sulfidation product.

## Results and Discussion

Sulfidation of 2 grams of nickel-manganese-cobalt oxide (NMC) lithium ion battery cathode was conducted following the methodology above, at 1000 °C and a  $P_{S_2}/P_{SO_2}$  ratio of approximately 10,  $P_{S_2}$  of approximately 0.1 atm. As determined from the rate of oxygen liberation in the form of  $SO_2$ , the reaction rate became kinetically negligible after about 50 minutes. This was taken to be the point at which the NMC reached a quasi-equilibrium with the  $S_2/SO_2$  atmosphere, upon which the sulfur flow was stopped and the furnace cooled. Under such conditions, nickel, cobalt, and manganese were thermodynamically predicted to form sulfides, while lithium was predicted to form a sulfate (Figure 1b). As observed through energy dispersion spectroscopy (EDS), nickel and cobalt from the NMC oxide were indeed sulfidized (Figure 2). Surprisingly, manganese from the NMC oxide did not fully sulfidize, forming instead a separate oxysulfide phase. At 1000 °C, nickel sulfide and cobalt sulfide are reported to form a fully miscible liquid<sup>19</sup>. While nickel and cobalt sulfides did melt, they were observed in this study to phase separate into distinct cobalt-rich and nickel-rich liquid sulfides. The nickel-rich sulfide, cobalt-rich sulfide, and manganese oxysulfide phases coalesced into single phase regions on the order of 100  $\mu m$  to 1 mm in size during the sulfidation reaction. While the distribution of lithium was unobservable post sulfidation with EDS, x-ray diffraction (XRD) revealed that lithium existed largely as a sulfate.

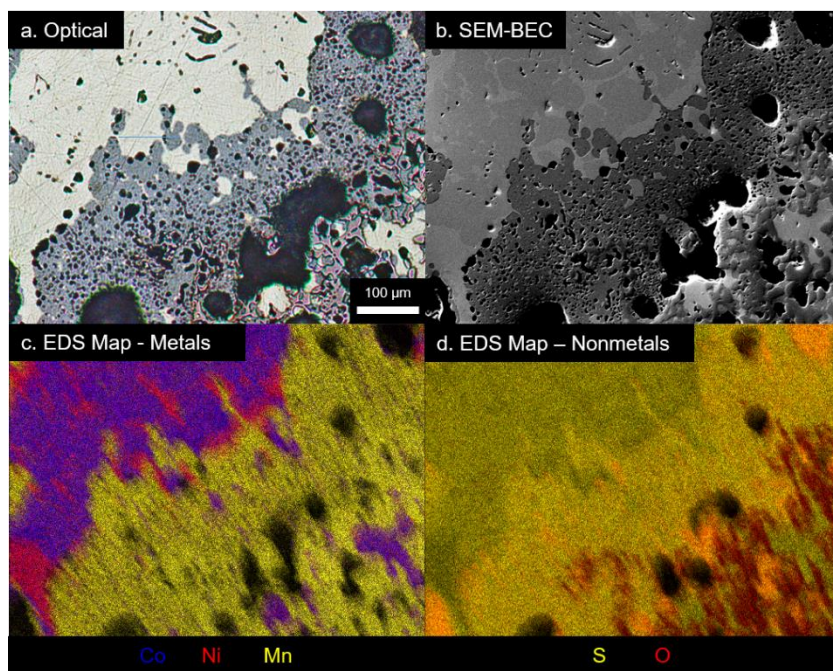


**Figure 2: Lithium, nickel, manganese, and cobalt were selectivity sulfidized from synthetic nickel-manganese-cobalt oxide cathode material.** Optical microscopy (a), SEM microscopy (b), and EDS mapping (c,d) reveal that upon selective sulfidation, a cobalt-rich sulfide (c, purple,  $Co_{0.67}Ni_{0.33}S$ ), nickel-rich sulfide (c, pink,  $Ni_{0.75}Co_{0.25}S$ ), and manganese oxysulfide (c, yellow,  $MnO_{0.2}S_{0.8}$ ) phases formed. These phases coalesced to sizes between 100  $\mu m$  and 1 mm, suggesting that nickel, manganese, and cobalt may be liberated via comminution and physical separation. Minimal inclusion between manganese and nickel-cobalt is observed. While lithium is indiscernible on the EDS maps, XRD reveals lithium to exist as a sulfate, suggesting oxygen-rich regions in (c,d) lacking Ni, Mn, or Co may correspond to lithium sulfate. Due to differences in aqueous solubilities between sulfides, oxysulfides, and sulfates, lithium may be potentially recovered from sulfidized metals via leaching.

Starting from synthetic NMC oxide cathode material, the sulfidation treatment resulted in the selective sulfidation of nickel and cobalt to sulfides, manganese to oxysulfide, and lithium to sulfate. Furthermore, not only was sulfidation conducted selectively, but the resultant nickel-rich sulfide, cobalt-

rich sulfide, and manganese oxysulfide coalesced into large phases  $>100\text{ }\mu\text{m}$ , large enough to support practical liberation of nickel and cobalt from manganese via comminution alone<sup>20</sup>. The differing hydrophobicity of sulfides and oxysulfides suggest that nickel and cobalt may therefore be isolated from manganese using flotation<sup>21</sup>. Meanwhile the soluble nature of alkali metal sulfates in water, in contrast to the largely insoluble behavior of transition metal oxides, oxysulfides, and sulfides, suggests that lithium can possibly be selectively leached and recovered from selectively sulfidized lithium ion battery cathodes. Indeed, selective sulfidation of lithium-nickel-manganese-cobalt oxide may facilitate the isolation of nickel-cobalt, manganese, and lithium, a promising avenue for recycling of lithium ion batteries. For isolation of cobalt from nickel, some preliminary separation is possible during selective sulfidation due to the immiscibility of the cobalt-rich and nickel-sulfide liquids. Following, selective molten sulfide electrolysis was explored as a complementary avenue to integrate cobalt and nickel separation and reduction into a single processing step.

## Selective Electrowinning of Nickel and Cobalt from Molten Sulfides

### *Experimental*

For selective electrowinning of nickel and cobalt from liquid sulfides, the electrolyte consisted of nickel sulfide ( $\text{Ni}_3\text{S}_2$ , 99.7% metals basis purity, Sigma Aldrich) cobalt sulfide ( $\text{CoS}$ , 99.5% metals basis purity, Fisher Scientific), barium sulfide ( $\text{BaS}$ , 99.7% metals basis purity, Alfa Aesar), and lanthanum sulfide ( $\text{La}_2\text{S}_3$ , 99.5% metals basis purity, Strem Chemical) at a composition of  $(\text{Ni}_3\text{S}_2)_7(\text{CoS})_{21}(\text{BaS})_{54}(\text{La}_2\text{S}_3)_{15}$ . The  $(\text{BaS})_{54}(\text{La}_2\text{S}_3)_{15}$  supporting electrolyte has recently been shown to increase the ionic transference number of molten transition metal sulfides<sup>15</sup>, making them suitable for electrolytic decomposition. While the phase stability of some transition metal sulfides in the  $\text{BaS}$ - $\text{La}_2\text{S}_3$  supporting electrolyte is known<sup>15,16</sup>, the liquidus behavior of mixed  $\text{Ni}_3\text{S}_2$ ,  $\text{CoS}$ ,  $\text{BaS}$ , and  $\text{La}_2\text{S}_3$  remains unclear. Therefore, a sample of the electrolyte was held at  $1500\text{ }^\circ\text{C}$  for one hour to confirm that the electrolyte formed a stable liquid at temperatures necessary for liquid nickel and cobalt deposition. To understand the electrochemical behavior of the electrolyte, open circuit potential (OCP), potentiostatic electrochemical impedance spectroscopy (EIS), and cyclic voltammetry (CV) were performed on the liquid  $(\text{Ni}_3\text{S}_2)_7(\text{CoS})_3(\text{BaS})_{54}(\text{La}_2\text{S}_3)_{15}$  at  $1500\text{ }^\circ\text{C}$  using a potentiostat/galvanostat (Reference 3000, Gamry) with a three electrode cell constructed in-house from an alumina crucible, with cell design and electrode orientation described elsewhere<sup>14,15</sup>. Galvanostatic electrolysis was also conducted at an anodic current density of  $1.5\text{ A/cm}^2$  using the same cell, reconfigured with two electrodes similarly described elsewhere<sup>14,15</sup>. All electrodes were machined in-house from EDM graphite (Isostatically Pressed, EC-12 / AC-12, Tokai Carbon). The cell was operated within the hot zone of a tube furnace (SS15R-2.50X6V-1Z, Mellen) inside of an alumina tube of 64mm OD, 58mm ID, under inert atmosphere with an argon ( $\text{Ar}$ , 99.95% purity, Air Gas) flowrate of 400 sccm. Post-electrolysis, the electrolyte was mounted in epoxy, cross sectioned, polished, and then imaged optically and via scanning electron microscope (SEM, JEOL JSM-6610LV, JEOL Ltd.) equipped with an energy dispersion spectroscopy analyzer (EDS, Sirius SD detector, SGX Sensortech Ltd.).

### *Results and Discussion*

Due to the unexplored nature of the  $(\text{Ni}_3\text{S}_2)_7(\text{CoS})_{21}(\text{BaS})_{54}(\text{La}_2\text{S}_3)_{15}$  electrolyte, the liquid phase stability was tested by holding a sample of the electrolyte in an alumina crucible at the electrolysis operating temperature of  $1500\text{ }^\circ\text{C}$  for one hour. Once cooled, the sample was observed to have melted and wetted the alumina, with less than 1% mass loss observed. Following, the electrolytic nature of the molten sulfide was explored using a three electrode cell with graphite working, counter, and quasi-reference electrodes as described previously. Before electrochemical measurements, the melt was held at the operating temperature of  $1500\text{ }^\circ\text{C}$  for one hour. The electrodes were confirmed to be in contact with the electrolyte by measuring the open circuit potential (OCP). The cell resistance between the working and quasi-reference electrodes (WE, quasi-RE) with a 4 cm separation was found through electrochemical impedance spectroscopy (EIS) to be  $0.5\text{ }\Omega$ . Cyclic voltammetry was conducted at a scan rate of  $5\text{ mV per second}$  with a potential sweep between  $+1.5\text{ V}$  to  $-1.5\text{ V}$  vs the quasi-RE (Figure 3a). Reported potentials

depicted in voltammetric data have been corrected post-measurement by 80% of the EIS-measured solution resistance between the graphite WE and quasi-RE. At very positive potentials, the anodic current showed noise that is characteristic of fluctuating cell resistance, typically due to gas evolution<sup>14,15,22</sup>. As the potential sweep moved to negative values, two current peaks are observed at current densities between -1.3 and -1.5 A/cm<sup>2</sup>, likely corresponding to nickel sulfide and cobalt sulfide reduction. The potential difference between the two peaks was observed to be approximately 140 mV. Galvanostatic electrolysis was conducted for 3750 seconds at an anodic current density of 1.5 A/cm<sup>2</sup>, corresponding to the upper bound of current density at which the two faradic events were observed during CV (Figure 3b). As shown in Figure 3c, the applied voltage shows rapid fluctuations with a period on the order of a second. This is attributed to changing cell resistance during electrolysis due to evolution of sulfur gas bubbles on the anode<sup>14,15,22</sup>.

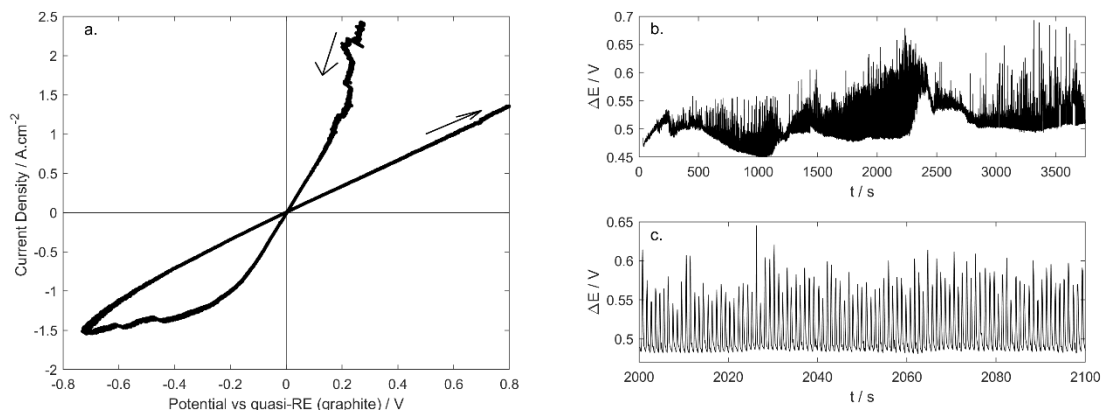


**Figure 3: Cyclic voltammetry and galvanostatic electrolysis suggest the presence of faradaic events corresponding to metal reduction and gas evolution.** a. During cyclic voltammetry analysis of the molten (Ni<sub>3</sub>S<sub>2</sub>)(CoS)<sub>3</sub>(BaS)<sub>54</sub>(La<sub>2</sub>S<sub>3</sub>)<sub>15</sub> at 1500 °C at a scan rate of 5 mV/s, fluctuations during high anodic current densities suggest sulfur gas evolution, while peaks at high cathodic current densities suggest nickel and cobalt metal reduction show a potential difference of approximately 140 mV. Reported potentials depicted in voltammetric data have been corrected post-measurement by 80% of the EIS-measured solution resistance (0.5 Ω) between the graphite working and quasi-reference electrodes. b. Bulk galvanostatic electrolysis of (Ni<sub>3</sub>S<sub>2</sub>)(CoS)<sub>3</sub>(BaS)<sub>54</sub>(La<sub>2</sub>S<sub>3</sub>)<sub>15</sub> at current densities observed to facilitate faradic events revealed recurring fluctuations in cell potential versus time, attributed changing solution resistance due to sulfur gas evolution at the anode. c. Fluctuations during bulk galvanostatic electrolysis of (Ni<sub>3</sub>S<sub>2</sub>)(CoS)<sub>3</sub>(BaS)<sub>54</sub>(La<sub>2</sub>S<sub>3</sub>)<sub>15</sub> occurred with a period of approximately 1 second.

Post electrolysis, the electrolyte was mounted in epoxy and examined under optical and scanning electron microscopes (Figure 4). The electrolyte was observed to wet both the alumina crucible and the graphite electrodes. Metal droplets on the order of 10-100 μm were observed in a cloud near the graphite cathode, decreasing in frequency toward the graphite anode. EDS analysis revealed the metal to have a composition of approximately 64 at% Co, 34 at% Ni, 2 at% S, illustrating that cobalt was selectively reduced from mixed, equimolar (metal basis), cobalt-nickel sulfide via molten sulfide electrolysis in the barium sulfide / lanthanum sulfide supporting electrolyte. Cobalt-rich sulfide phases of approximately the same cobalt-nickel ratio, free of lanthanum and barium sulfide, were observed surrounding the reduced metal, suggesting that post-electrolysis, the reduced metal may have back-reacted with dissolved sulfur gas in the system. The presence of residual sulfur in the system is of no surprise, considering the solubility for sulfur gas previously observed in liquid barium-lanthanum sulfide-containing systems<sup>22</sup>. The successful reduction of cobalt and nickel metal from the molten sulfide at current densities observed in CV to correspond with faradic events suggests the two peaks 140 mV apart observed in Figure 3a correspond to cobalt and nickel reduction. This 140 mV difference in decomposition potential of nickel



sulfide and cobalt sulfide in the barium-lanthanum sulfide suggests that molten sulfides are candidate electrolytes for selective reduction of difficult to separate metals.

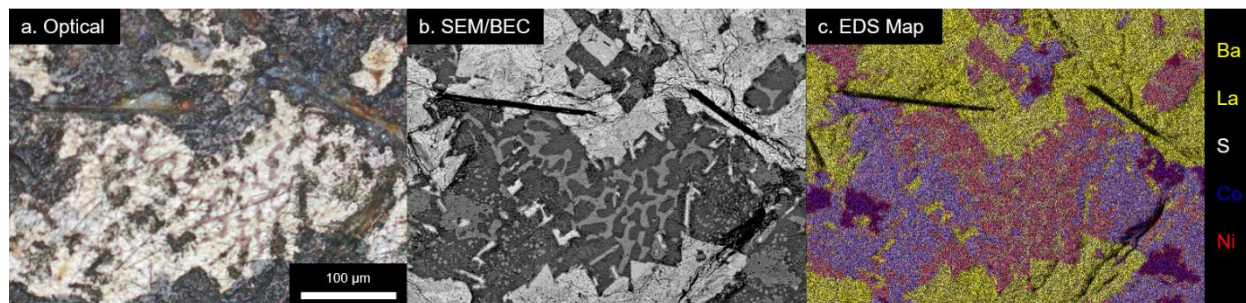


**Figure 4: Molten sulfide electrolytes support selective electrowinning of cobalt from nickel.** Optical microscopy (a), SEM microscopy (b), and EDS mapping (c) reveal cobalt and nickel reduction at a composition of 64 at% Co, 34 at% Ni, and 2 at% S (dark blue) from equimolar (metal basis) Ni-Co-S in a Ba-La-S supporting electrolyte. Sulfide regions of similar metal composition to the reduced metal (light blue) surround the cobalt-nickel alloy, suggesting that back-reaction of cobalt-nickel to sulfide may have occurred post-electrolysis during cooling and solidification.

## Conclusions

Herein, we demonstrate that for simulated nickel-manganese-cobalt oxide cathode material, selective sulfation results in the formation of lithium sulfate, manganese oxysulfide, and cobalt-nickel sulfide. During the selective sulfidation process, manganese oxysulfide and nickel-cobalt sulfides each coalesced into single-phase regions on the order of 100 µm – 1mm in size, large enough for practical recovery via comminution and physical separation. The existence of lithium as a sulfate suggests that it may be recovered from the other insoluble metal compounds via leaching. For isolation and reduction of cobalt from the mixed nickel-cobalt sulfides, we demonstrate selective molten sulfide electrolysis at 1500 °C, employing barium-lanthanum sulfide as a supporting electrolyte. Many promising electrochemical engineering avenues exist to optimize selective electrowinning of nickel and cobalt from molten sulfides, including the employment of liquid cathodes and the optimization of sulfide electrolytes and operating conditions. These process parameters may be informed and optimized through studies of thermodynamics, mass transport, and electrochemical kinetics in molten sulfide systems. Even now, crude, un-optimized selective sulfidation and molten sulfide electrolysis present a promising avenue for lithium ion battery recycling, particularly for complicated waste streams containing nickel-manganese-cobalt oxide cathodes. Selective sulfidation as demonstrated herein suggests that oxide-sulfide anion exchange chemistry is a tenable tool for challenging metal separations. Meanwhile selective molten sulfide electrolysis facilitates process intensification by combining separation and reduction operations for difficult to separate metals, such as nickel and cobalt, into a single unit operation.

## References

- Olivetti, E. A., Ceder, G., Gaustad, G. G. & Fu, X. Lithium-Ion Battery Supply Chain Considerations: Analysis of Potential Bottlenecks in Critical Metals. *Joule* **1**, 229–243 (2017).
- Harper, G. *et al.* Recycling lithium-ion batteries from electric vehicles. *Nature* **575**, 75–86 (2019).
- Ciez, R. E. & Whitacre, J. F. Examining different recycling processes for lithium-ion batteries. *Nat. Sustain.* **2**, 148–156 (2019).
- Wang, M. & Navrotsky, A. Enthalpy of formation of LiNiO<sub>2</sub>, LiCoO<sub>2</sub> and their solid solution, LiNi<sub>1-x</sub>Co<sub>x</sub>O<sub>2</sub>. *Solid State Ionics* **166**, 167–173 (2004).
- Chang, K., Hallstedt, B. & Music, D. Thermodynamic and Electrochemical Properties of the Li–Co–O and Li–Ni–O Systems. *Chem. Mater.* **24**, 97–105 (2011).
- Piskunen, P. *et al.* Precious Metal Distributions in Direct Nickel Matte Smelting with Low-Cu Mattes. *Metall. Mater. Trans. B Process Metall. Mater. Process. Sci.* **49**, 98–112 (2018).



7. Gaballah, I. & Djona, M. Recovery of Co, Ni, Mo, and V from Unroasted Spent Hydrotreating Catalysts by Selective Chlorination. *Metall. Mater. Trans. B* **26B**, 41–50 (1995).
8. Zante, G. *et al.* Solvent extraction fractionation of manganese, cobalt, nickel and lithium using ionic liquids and deep eutectic solvents. *Miner. Eng.* **156**, 106512 (2020).
9. Dhiman, S. & Gupta, B. Partition studies on cobalt and recycling of valuable metals from waste Li-ion batteries via solvent extraction and chemical precipitation. *J. Clean. Prod.* **225**, 820–832 (2019).
10. Harris, C. T., Peacey, J. G. & Pickles, C. A. Selective sulphidation and flotation of nickel from a nickeliferous laterite ore. *Miner. Eng.* **54**, 21–31 (2013).
11. Korkmaz, K., Alemrajabi, M., Rasmuson, Å. & Forsberg, K. Recoveries of Valuable Metals from Spent Nickel Metal Hydride Vehicle Batteries via Sulfation, Selective Roasting, and Water Leaching. *J. Sustain. Metall.* **4**, 313–325 (2018).
12. Shi, J. *et al.* Sulfation Roasting Mechanism for Spent Lithium-Ion Battery Metal Oxides Under SO<sub>2</sub>-O<sub>2</sub>-Ar Atmosphere. *JOM* **71**, 4473–4481 (2019).
13. Stinn, C. & Allanore, A. Estimating the Capital Costs of Electrowinning Processes. *Electrochem. Soc. Interface* **29**, 44–49 (2020).
14. Sokhanvaran, S., Lee, S.-K., Lambotte, G. & Allanore, A. Electrochemistry of Molten Sulfides: Copper Extraction from BaS-Cu<sub>2</sub>S. *J. Electrochem. Soc.* **163**, D115–D120 (2016).
15. Sahu, S. K., Chmielowiec, B. & Allanore, A. Electrolytic Extraction of Copper, Molybdenum and Rhenium from Molten Sulfide Electrolyte. *Electrochim. Acta* **243**, 382–389 (2017).
16. Stinn, C., Nose, K., Okabe, T. & Allanore, A. Experimentally Determined Phase Diagram for the Barium Sulfide-Copper(I) Sulfide System Above 873 K (600 °C). *Metall. Mater. Trans. B* **48**, 2922–2929 (2017).
17. Afanasiev, P. *et al.* Preparation of the mixed sulfide Nb<sub>2</sub>Mo<sub>3</sub>S<sub>10</sub> catalyst from the mixed oxide precursor. *Catal. Letters* **64**, 59–63 (2000).
18. Meyer, B. Elemental sulfur. *Chem. Rev.* **76**, 367–388 (1976).
19. Jacob, K. T. Isothermal Section of the Ni-Co-S Phase Diagram at 1273 K. *Metall. Trans. B* **11B**, 640–643 (1980).
20. Gallios, G. P., Kyzas, G. Z. & Matis, K. A. Flotation in the 2010s: Focus on mineral processing. in *Advanced Low-Cost Separation Techniques in Interface Science* **30**, 43–68 (Elsevier B.V., 2019).
21. Kyzas, G. Z., Lazaridis, N. K. & Matis, K. A. Flotation: Recent innovations in an interesting and effective separation process. in *Advanced Low-Cost Separation Techniques in Interface Science* **30**, 15–42 (Elsevier B.V., 2019).
22. Chmielowiec, B. J. *Electrochemical Engineering Considerations for Gas Evolution in Molten Sulfide Electrolytes*. (Massachusetts Institute of Technology, 2019).